

Supporting Information

Guest-Induced SC-SC Transformation within the First K/Cd Heterodimetallic Triazole Complex: a Luminescent Sensor for High- Explosive and Cyano Molecules

Ying Wang,* Wei Jia, Ran Chen, Xiao-Jun Zhao*, and Zhong-Liang Wang*

1. Synthesis of 1,1,2,2-tetrakis[4-(1H-1,2,4-triazol-1-yl)phenyl]-ethylene (TTPE)

TTPE ligand was synthesized according to literature methods.^{S1} A mixture of 1,1,2,2-tetrakis(4-bromophenyl)ethene (1.77 g, 2.74 mmol), 1H-1,2,4-triazole (0.757 g, 10.96 mmol), potassium carbonate (0.76 g, 5.48 mmol), and CuO (0.01 g, 0.125 mmol) was heated with stirring in DMSO (15 mL) at 150°C for 48 h. The resulting slurry was cooled to room temperature, and solids were removed by filtration. DMSO in the filtrate was removed by distillation under reduced pressure. Dichloromethane was added to the remaining filtrate, and the mixture was then washed with water and dried over sodium sulfate. Then the solvent dichloromethane was removed. The products were crystallized in methanol and water, and yellow block single crystals suitable for X-ray diffraction were obtained by slow evaporation of the solvents within two days. Yield: 18%. M.p. 253-255 °C; FTIR: ν = 3340 (bm), 1647 (s), 1533 (s), 1385 (m), 1277 (m), 1093 (s), 979 (m), 873 (m), 687 (w), 617 (w), 539 cm^{-1} (m).

2. Synthesis of Complex 1

1 was prepared by the reaction of $\text{Cd}(\text{NO}_3)_2 \cdot 4\text{H}_2\text{O}$ (0.4 mmol), TTPE (0.1 mmol), and HCOOH (0.2 mmol) in a $\text{H}_2\text{O}/\text{CHCl}_3/\text{CH}_3\text{OH}/\text{DMAC}$ solution. After stirring for about half an hour, the resulting solution was filtered. Light yellow single crystals suitable for X-ray diffraction were obtained by slow evaporation of the solvents with 60% yield based on $\text{Cd}(\text{NO}_3)_2 \cdot 4\text{H}_2\text{O}$. Anal. Calcd for $\text{C}_{43}\text{H}_{45}\text{CdN}_{15}\text{O}_8$: C, 51.02; H, 4.48; N, 20.75. Found: C, 51.09; H, 4.52; N 20.77.

3. Synthesis of Complex 1a

1 (1 mmol) were immersed into an aqueous solution for 3 days. Complex **1** maintained crystallinity throughout. There was no apparent change in the shape and color of the crystals. Block yellow single crystals suitable for X-ray diffraction were obtained with 30% yield based on **1**. Anal. Calcd for C₆₈H₅₆CdN₂₆O₁₀: C, 54.10; H, 3.74; N, 24.12. Found: C, 54.01; H, 3.83; N 24.15.

4. Synthesis of Complex 1b

1 (1 mmol) were immersed into an aqueous solution of KCl for 6 h. Complex **1** maintained crystallinity throughout. There was no apparent change in the shape and color of the crystals. Block yellow single crystals suitable for X-ray diffraction were obtained with 20% yield based on **1**. Anal. Calcd for C₁₀₂H₉₈Cd₃Cl₆K₂N₃₆O₁₂: C, 46.26; H, 3.73; N, 19.04. Found: C, 46.31; H, 3.80; N 19.09.

5. Solvent-Dependent Luminescence

The fine grinding sample **1** (2.5 mg) or **1a** (3.0 mg) was immersed in different organic solvents (5 mL), treated by ultrasonication for 30 min and then aged for 3 days to form a stable emulsion. The used solvents are alcohols (methanol, ethanol, *n*-propanol, and 2-propanol), ketones (acetone), amides (N,N'-dimethylacetamide (DMAC)), nitriles (CH₃CN), chloroalkanes (CH₂Cl₂, and CHCl₃), nitro-aromatics (1,3-dinitrobenzene (*m*-DNB), 1,4-dinitrobenzene (*p*-DNB), 1-fluoro-4-nitrobenzene (FNB), nitrobenzene (NB)), nitro-aliphatic (nitromethane (NM), and tris(hydroxymethyl)nitromethane (THMNM)), and even other aromatic complexes and heterocycles (toluene, pyridine, morpholine). As shown in Fig. S8, the intensities of the emission spectra are largely dependent on the solvent molecules, particularly in the case of *p*-DNB, which exhibited the most quenching.

5. The Luminescence Sensing of Complexes 1 and 1a on Metal Ions

Though our research interest focused on the detecting of nitro-aromatics and similar pollutions and explosives, additional experiments were performed to preliminarily investigate the potential of this MOFs in ion sensing. Cd²⁺, Ca²⁺, Co²⁺, Mg²⁺, Ni²⁺, Zn²⁺ (metal chloride) were tested. The fluorescence spectroscopic studies were carried out with the addition of 0-3 equiv different metal chloride into the DMF solution of **1**

with 5×10^{-4} M. As shown in Fig. S12, a luminescence increase was observed upon the addition of Ca^{2+} ions. The highest band at about 500 nm is ca. twice as intense as the corresponding peak in DMF solution without Ca^{2+} ions. To further understand this experimental phenomenon, the same experiments were made with the introduction of Cd^{2+} (CdCl_2), Co^{2+} ions (CoCl_2), Mg^{2+} (MgCl_2), Ni^{2+} ions (NiCl_2), and Zn^{2+} (ZnCl_2) into the systems. It is interesting that, upon adding Mg^{2+} ions, the emission intensity of **1** exhibits almost the same intensity as that seen for **1**. While the addition of Ni^{2+} , Co^{2+} , Cd^{2+} , and Zn^{2+} , the results exhibit that the luminescence peaks do not enhance, but rather the luminescent intensities of **1** are decreased. While the same procedure was made except that **1** was replaced by **1a**, the experimental results support the idea that the luminescent emission of **1a** shows excellent selectivity for Zn^{2+} ions, as shown in Fig. S13. Complexes **1** and **1a** may be further considered as luminescent probes of Ca^{2+} and Zn^{2+} , respectively.^{S2}

6. General Remarks

All the reagents are commercially available and used without further purification. The elemental analysis of Carbon, Nitrogen and Hydrogen has been measured on a Perkin-Elmer 240 elemental analyzer. Powder X-ray diffraction analysis has been determined on a D/Max-2500 X-ray diffractometer using $\text{Cu-K}\alpha$ radiation. The photoluminescence spectra have been recorded by a MPF-4 fluorescence spectrophotometer with a xenon arc lamp as the light source. The UV-vis spectra were obtained on a Jasco V-570 spectrophotometer. Thermal analyses (under an oxygenated atmosphere with a heating rate of $5\text{ }^\circ\text{C min}^{-1}$) were carried out in a Labsys NETZSCH TG 209 Setaram apparatus.

7. Crystallographic Studies

Single-crystal X-ray diffraction determination for complexes **1**, **1a** and **1b** have been collected on an APEX II CCD area detector. A graphite crystal monochromator was equipped in the incident beam for data collection at the temperature of 293(2) and 113.15 K. The ω - ϕ scan technique has been applied. Direct methods have been applied to solve the structures. Full-matrix least-squares methods using the SHELXL-97 and SHELXS-97 programs have been used to refine the crystal structures.^{S3,S4} For

all the coordination complexes anisotropic thermal parameters have been applied to all non-hydrogen atoms. Anomalous dispersion corrections have been incorporated and analytical expressions of neutral-atom scattering factors were also used. These crystallographic data, selected bond distances and bond angles of these title complexes are listed in Table S1 and Table S2, respectively. The crystallographic data for this paper have been assigned to the following deposition CCDC number as CCDC- 1506062 (**1**), 1506063 (**1a**), and 1451843 (**1b**). These data can be obtained free of charge from The Cambridge Crystallographic Data Centre via www.ccdc.cam.ac.uk/data_request/cif.

8. Luminescent Sensor for *p*-DNB

To further investigate the sensing properties of **1** and **1a**, the emissive response is monitored by gradually increasing *p*-DNB contents of the emulsions of **1** and **1a** dispersed in DMF. As shown in Fig. S10, the emission intensity decreased upon the addition of *p*-DNB with 5 ppm and was nearly completely quenched at the concentration of 150 ppm with a high quenching efficiency of 96.91 and 97.65%, which is higher than or comparable to other MOF sensors for NB.^{S5} As illustrated in Fig. S11, compared to the other nitro-aromatics, both **1** and **1a** are more sensitive to *p*-DNB with a high quenching efficiency of 99.92 and 99.81%, respectively. Also, the quenching phenomenon of **1** and **1a** in the solid state is consistent with that realized in the liquid sensing process, indicating that the quenching mechanism should be based on the nature of the complex rather than the testing environments.

9. Thermal Stability of **1** and **1a**

1 and **1a** possess high thermal stability, confirmed by thermal gravimetric analysis (TGA) on crystalline samples of these compounds in the range from 32 to 700 °C. The TGA results reveal that both complexes did not decompose until 400 °C (Fig. S16, ESI†).

References

S1 Y. Wang, B. Yuan, Y.-Y. Xu, X.-G. Wang, B. Ding and X.-J. Zhao, *Chem. Eur. J.* 2015, **21**,

2107.

- S2 (a) J.-Y. Liu, Q. Wang, L.-J. Zhang, B. Yuan, Y.-Y. Xu, X. Zhang, C.-Y. Zhao, D. Wang, Y. Yue, Y. Wang, B. Ding, X.-J. Zhao and M. M. Yue, *Inorg. Chem.* 2014, **53**, 5972; (b) Y. Wang, B. Yuan, Y.-Y. Xu, X.-G. Wang, B. Ding and X.-J. Zhao, *Chem. Eur. J.* 2015, **21**, 2107; (c) D. Sun, H. R. Xu, C. F. Yang, Z. H. Wei, N. Zhang, R. B. Huang and L. S. Zheng, *Cryst. Growth Des.* 2010, **10**, 4642; (d) D. Sun, N. Zhang, R. B. Huang and L. S. Zheng, *Cryst. Growth Des.* 2010, **10**, 3699; (e) B. Zhao, H. L. Gao, X. Y. Chen, P. Cheng, W. Shi, D. Z. Liao, S. P. Yan and Z. H. Jiang, *Chem. Eur. J.* 2006, **12**, 149; (f) B. Zhao, X.-Y. Chen, P. Cheng, D.-Z. Liao, S.-P. Yan and Z.-H. Jiang, *J. Am. Chem. Soc.* 2004, **126**, 15394.

S3 SHELXS 97, Program for the Solution of Crystal Structures; G. M. Sheldrick, Ed., University of Göttingen: Göttingen, Germany, 1997.

S4 SHELXL 97, Program for the Refinement of Crystal Structures; G. M. Sheldrick, Ed. University of Göttingen: Göttingen, Germany, 1997.

S5 (a) D. Tian, R.-Y. Chen, Z. Chang, G.-Y. Wang and X.-H. Bu, *J. Mater. Chem. A* 2014, **2**, 1465;

(b) S. Pramanik, C. Zheng, X. Zhang, T. J. Emge, J. Li, *J. Am. Chem. Soc.* 2011, **133**, 4153; (c)

S. S. Nagarkar, B. Joarder, A. K. Chaudhari, S. Mukherjee and S. K. Ghosh, *Angew. Chem., Int. Ed.* 2013, **52**, 2881.

Table S1 Crystallographic Data and Details of Refinements for Complexes **1**, **1a**, and **1b**.

	1	1a	1b				
formula	C ₄₃ H ₄₅ CdN ₁₅ O ₈	C ₆₈ H ₅₆ CdN ₂₆ O ₁₀	C ₁₀₂ H ₉₈ Cd ₃ Cl ₆ K ₂ N ₃₆ O ₁₂				
<i>M</i> (g mol ⁻¹)	1012.32	1509.75	2648.26				
crystal system	triclinic	Monoclinic	Monoclinic				
space group	<i>P</i> -1	<i>C</i> 2	<i>P</i> 2/ <i>c</i>				
temperature	293(2)	293(2)	113.15				
<i>a</i> (Å)	12.1538(9)	20.477(4)	16.136(3)				
<i>b</i> (Å)	12.1574(10)	23.839(5)	13.126(3)				
<i>c</i> (Å)	16.1536(14)	17.521(4)	34.238(7)				
<i>α</i> (°)	77.045(7)	90.00	90.00				
<i>β</i> (°)	82.550(7)	111.11(3)	90.19(3)				
<i>γ</i> (°)	83.527(7)	90.00	90.00				
<i>V</i> (Å ³)	2297.8(3)	7979(3)	7252(3)				
<i>Z</i>	2	4	2				
<i>F</i> (000)	1038	3164	2684				
ρ_{calc} (Mg m ⁻³)	1.460	1.299	1.213				
μ (mm ⁻¹)	0.544	0.596	0.663				
data/restraints/params	8106 / 0 / 628	18425 / 1 / 597	12543 / 42 / 773				
GOF on <i>F</i> ²	1.036	0.994	1.031				
<i>R</i> ₁ ^a (I=2σ(I))	0.0429	0.1097	0.1023				
ωR_2^a (all data)	0.1102	0.3095	0.2732				
^a <i>R</i> ₁	=	$\frac{\sum F_o }{\sum F_c }$	-	$\frac{ F_c }{ F_o }$	^b ωR_2	=	$[\frac{\sum w(F_o ^2 - F_c ^2)^2}{\sum w F_o ^2}]^{1/2}$

Table S2 Selected Bond Lengths [Å] and Angles [°] for Complexes **1**, **1a**, and **1b**.

1					
N(37)-Cd(1)#1	2.361(3)	N(42)-Cd(2)#1	2.301(3)	Cd(1)-N(46)	2.347(3)
Cd(1)-O(51)#2	2.276(2)	Cd(1)-N(37)#5	2.361(3)	Cd(2)-O(49)	2.300(2)
Cd(2)-N(42)#8	2.301(3)	Cd(2)-N(32)	2.383(3)	O(51)#2-Cd(1)-O(51)#3	180.00(12)
O(51)#2-Cd(1)-N(46)	90.84(10)	O(51)#3-Cd(1)-N(46)	89.16(10)	O(51)#3-Cd(1)-N(46)#4	90.84(10)
N(46)-Cd(1)-N(46)#4	180.000(1)	O(51)#2-Cd(1)-N(37)#5	80.23(10)	O(51)#3-Cd(1)-N(37)#5	99.77(10)
N(46)-Cd(1)-N(37)#5	89.62(10)	N(46)#4-Cd(1)-N(37)#5	90.38(10)	O(49)-Cd(2)-N(42)#8	88.70(10)
O(49)#7-Cd(2)-N(42)#8	91.30(10)	O(49)-Cd(2)-N(32)	87.82(9)	O(49)#7-Cd(2)-N(32)	92.18(9)
N(42)#8-Cd(2)-N(32)	93.28(10)	N(42)#6-Cd(2)-N(32)	86.72(10)	N(42)#8-Cd(2)-N(32)#7	86.72(10)
1a					
Cd(1)-O(3W)	2.233(12)	Cd(1)-N(8)	2.237(8)	Cd(1)-N(11)	2.315(9)
Cd(1)-N(6)#1	2.331(6)	Cd(1)-N(15)#2	2.339(11)	Cd(1)-O(2W)	2.353(10)
Cd(2)-O(4W)	2.02(2)	Cd(2)-N(24)#3	2.20(6)	Cd(2)-N(18)#4	2.32(4)
Cd(2)-N(20)	2.331(11)	Cd(2)-N(2)	2.347(11)	Cd(2)-O(1W)	2.366(12)
O(3W)-Cd(1)-N(8)	87.0(4)	O(3W)-Cd(1)-N(11)	91.3(3)	O(3W)-Cd(1)-N(6)#1	94.4(3)
N(8)-Cd(1)-N(11)	87.7(3)	N(11)-Cd(1)-N(6)#1	173.9(4)	O(3W)-Cd(1)-N(15)#2	90.0(4)
N(8)-Cd(1)-N(6)#1	90.6(3)	N(8)-Cd(1)-N(15)#2	176.2(4)	N(11)-Cd(1)-N(15)#2	90.1(4)
N(6)#1-Cd(1)-N(15)#2	92.0(3)	O(3W)-Cd(1)-O(2W)	177.9(5)	N(8)-Cd(1)-O(2W)	90.9(5)
N(11)-Cd(1)-O(2W)	88.5(3)	N(6)#1-Cd(1)-O(2W)	85.7(3)	N(15)#2-Cd(1)-O(2W)	92.1(5)
O(4W)-Cd(2)-N(24)#3	94(5)	O(4W)-Cd(2)-N(18)#4	91(2)	N(24)#3-Cd(2)-N(18)#4	90(6)
O(4W)-Cd(2)-N(20)	85.4(8)	N(24)#3-Cd(2)-N(20)	177(5)	N(18)#4-Cd(2)-N(20)	87(2)
O(4W)-Cd(2)-N(2)	89.7(7)	N(24)#3-Cd(2)-N(2)	94(5)	N(18)#4-Cd(2)-N(2)	176(2)
N(20)-Cd(2)-N(2)	89.0(4)	O(4W)-Cd(2)-O(1W)	171.3(9)	N(24)#3-Cd(2)-O(1W)	95(5)
N(18)#4-Cd(2)-O(1W)	89(2)	N(20)-Cd(2)-O(1W)	86.0(7)	N(2)-Cd(2)-O(1W)	89.4(5)
1b					
Cd1-N7	2.346(4)	Cd1-N1	2.364(3)	Cd1-N12	2.366(3)
Cd1-N6	2.361(4)	Cd1-Cl3	2.5943(15)	Cd1-Cl2	2.6362(19)
Cd2-N52	2.321(3)	Cd2-N13	2.349(3)	Cd2-Cl4	2.6020(13)
K3-Cl3	2.3600(18)	K3-O5	2.410(4)	K3-O6	2.449(4)
K3-O1	2.456(3)	N7-Cd1-N6	92.94(13)	N7-Cd1-N1	90.37(12)
N6-Cd1-N1	176.54(13)	N6-Cd1-N12	89.59(12)	N1-Cd1-N12	87.06(12)
N7-Cd1-Cl3	90.33(11)	N6-Cd1-Cl3	92.25(11)	N1-Cd1-Cl3	88.73(10)
N12-Cd1-Cl3	91.70(9)	N7-Cd1-Cl2	91.86(11)	N6-Cd1-Cl2	90.23(11)
N1-Cd1-Cl2	88.67(10)	N12-Cd1-Cl2	86.00(9)	Cl3-Cd1-Cl2	176.61(5)
N52-Cd2-N13	173.59(12)	N13-Cd2-Cl4	88.61(9)	Cl3-K3-O5	109.28(11)
Cl3-K3-O6	105.69(11)	O5-K3-O6	113.12(15)	Cl3-K3-O1	94.79(9)
O5-K3-O1	117.66(13)	O6-K3-O1	113.86(13)		

Symmetry transformations used to generate equivalent atoms: For **1**: #1 $x, y, z - 1$ #2 $-x + 1, -y, -z + 1$ #3 $x - 1, y + 1, z$ #4 $-x, -y + 1, -z + 1$ #5 $-x, -y + 1, -z$ #6 $x, y, z + 1$ #7 $-x + 2, -y, -z + 1$ #8 $-x + 2, -y, -z$ #9 $x + 1, y - 1, z$. For **1a**: #1 $x + 1/2, y + 1/2, z + 1$ #2 $x + 1, y, z$ #3 $x - 1/2, y - 1/2, z - 1$ #4 $x - 1, y, z$.

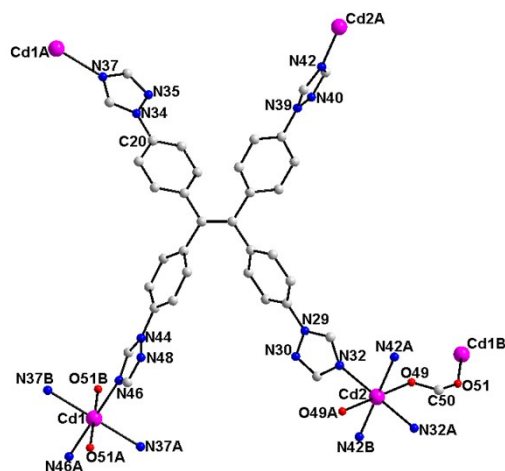


Fig. S1 The local coordination environments of the Cd centers and the ligands in **1**. Hydrogen atoms are omitted for clarity. Gray, C; blue, N; red, O; purple, Cd.

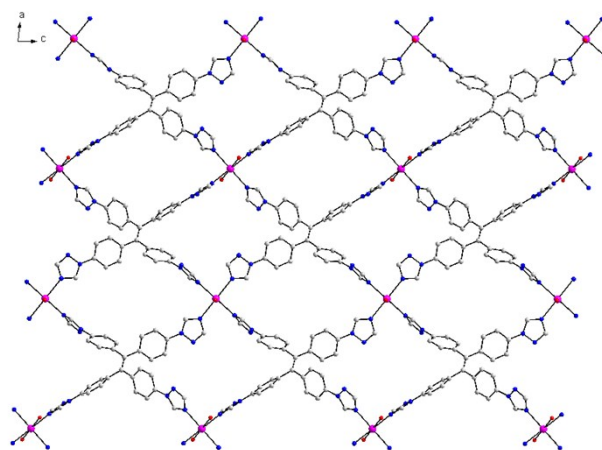


Fig. S2 The 2D layer of **1** connected by TTPE with Cd^{II} ions along *b* axis. Gray, C; blue, N; red, O; purple, Cd.

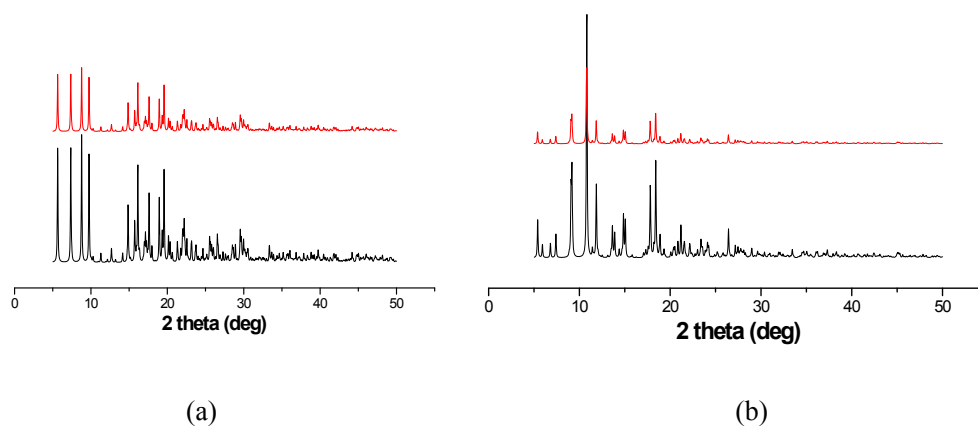


Fig. S3 PXRD patterns of **1** for (a) and **1a** for (b). Black, simulated; red, as-synthesized.

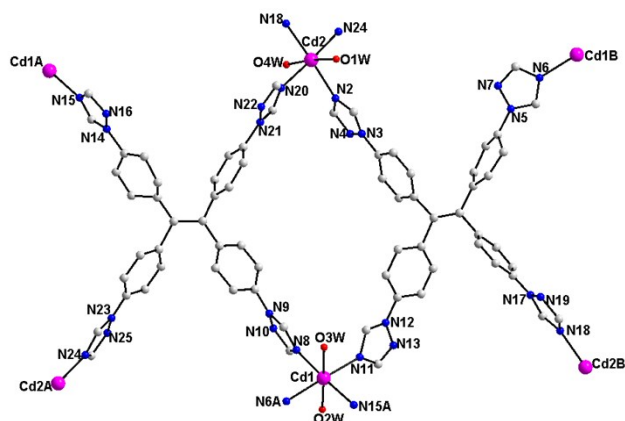


Fig. S4 The local coordination environments of the Cd^{II} centers and the ligands in **1a**. Hydrogen atoms are omitted for clarity. Gray, C; blue, N; red, O; purple, Cd.

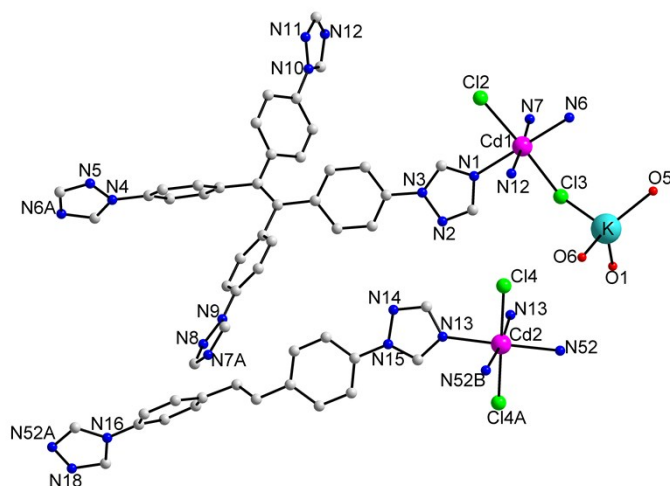


Fig. S5 The fundamental structural unit of **1b**. C gray, blue N, green, Cl; purple Cd; cyan K.

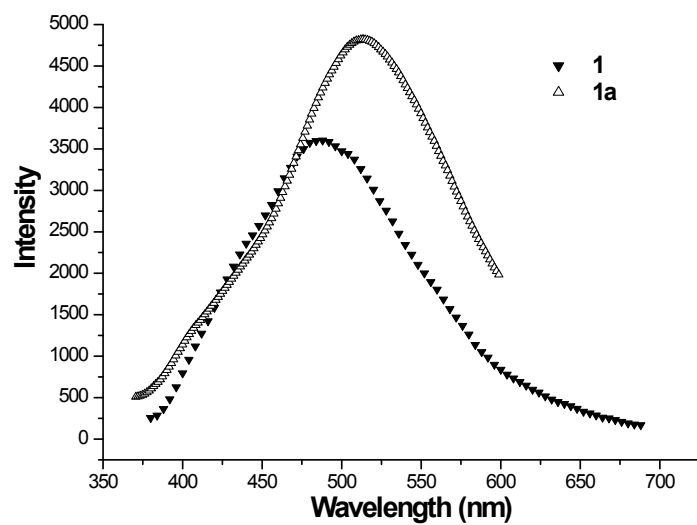


Fig. S6 Emission spectra of **1** and **1a** in DMSO solution at room temperature (5×10^{-4} mol/L for **1** and **1a**).

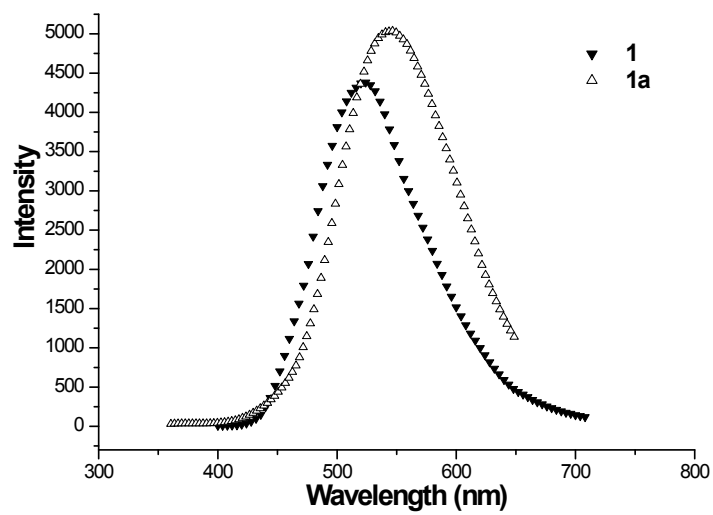
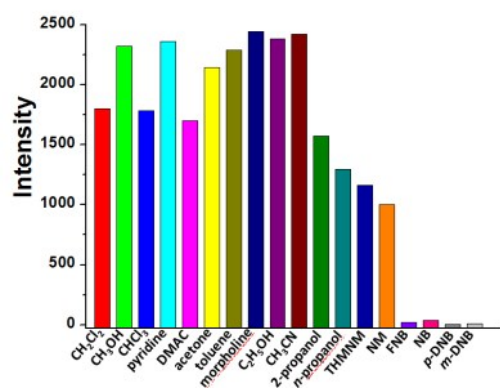
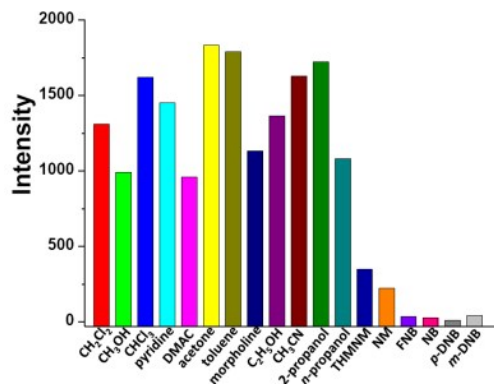


Fig. S7 Emission spectra of **1** and **1a** in solid state at room temperature.



(a)



(b)

Fig. S8 Emission intensity of **1** for (a) and **1a** for (b) dispersed in DMSO with the addition of different organics.

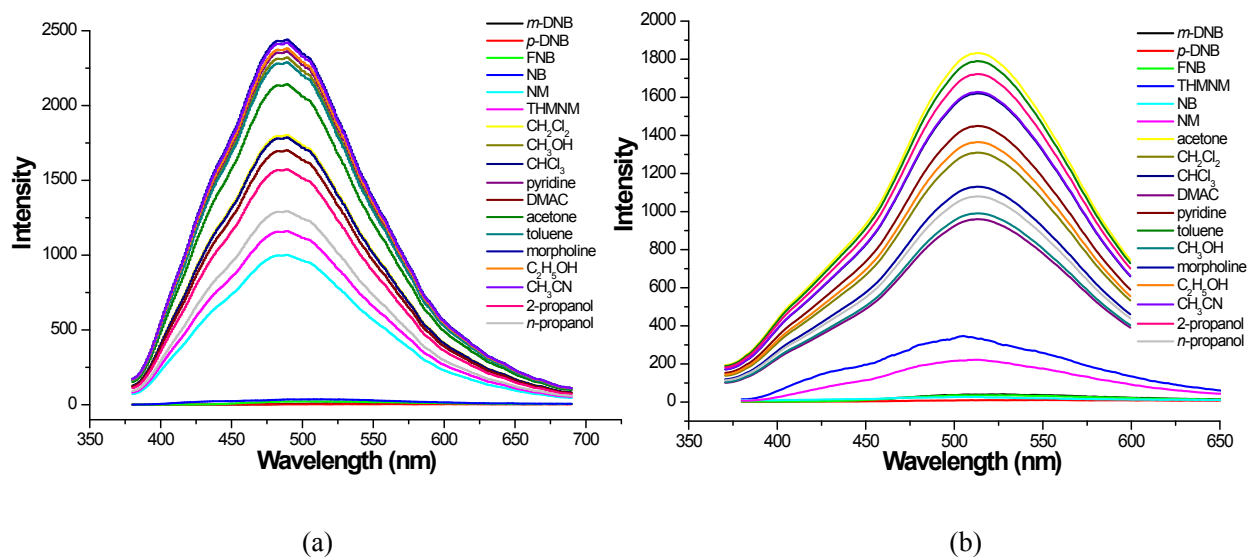
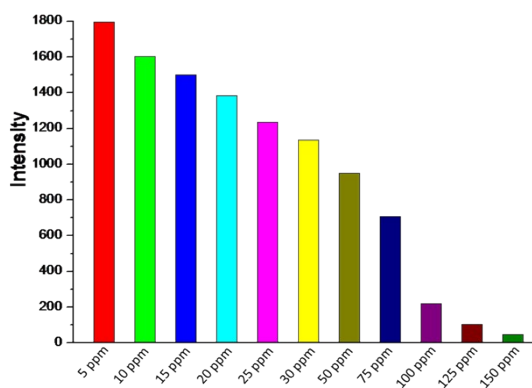
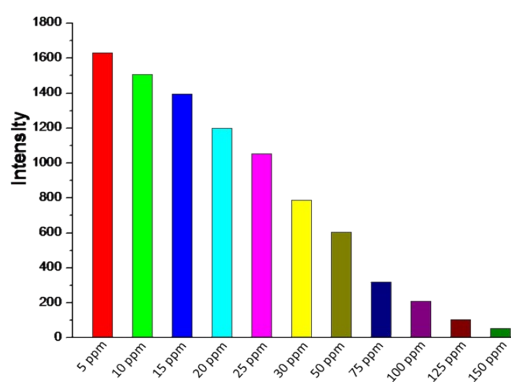


Fig. S9 Emission spectra of **1** for (a) and **1a** for (b) in different solvents.

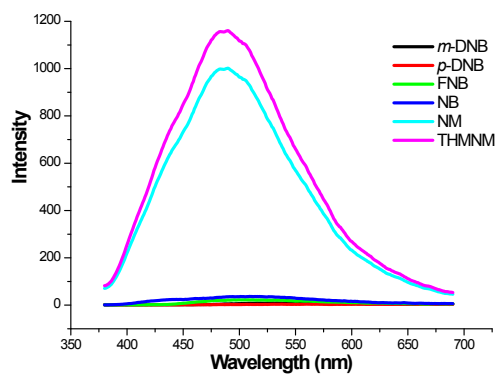


(a)

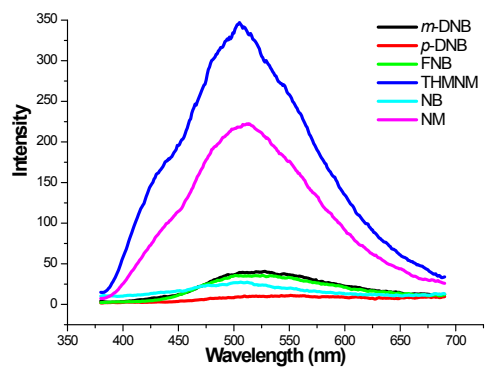


(b)

Fig. S10 Fluorescence titration intensity of complex **1** for (a), and **1a** for (b) dispersed in DMSO with the addition of different concentrations of *p*-DNB.



(a)



(b)

Fig. S11 Fluorescence titration of **1** for (a) and **1a** for (b) dispersed in six nitro-compounds with 2000 ppm.

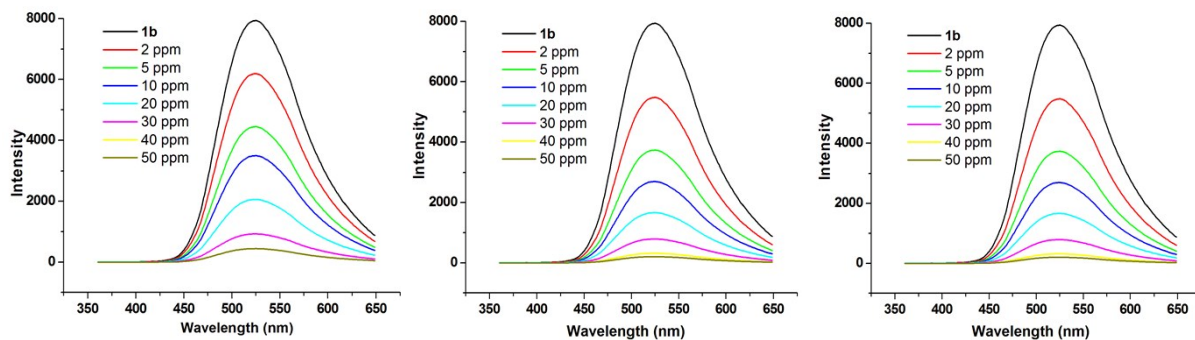
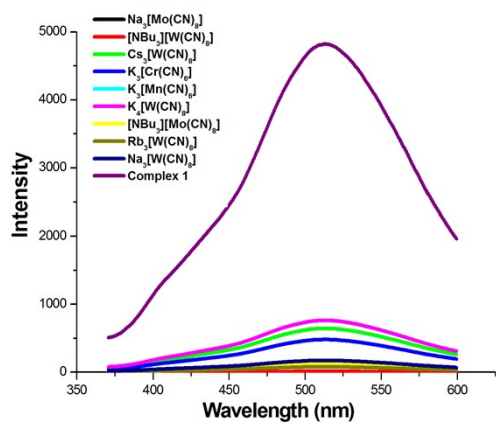
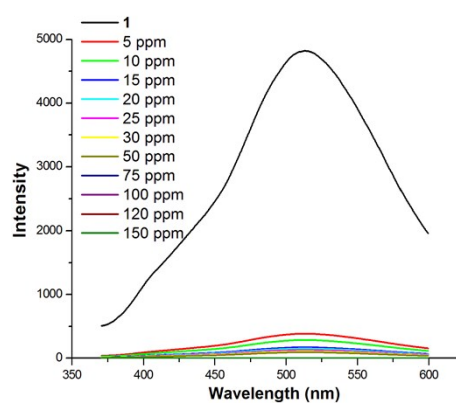


Fig. S12 Effect on the emission spectra of **1b** dispersed in DMSO upon incremental addition of a TNP for (a), TNT for (b), and CTT for (c) solution.



(a)



(b)

Fig. S13 (a) Emission spectra of **1b** dispersed in DMSO with the addition of different cyano-groups (400 ppm); (b) Fluorescence titration of complex **1b** dispersed in DMSO with the addition of different concentrations of $\text{Na}_3[\text{Mo}(\text{CN})_8]$.

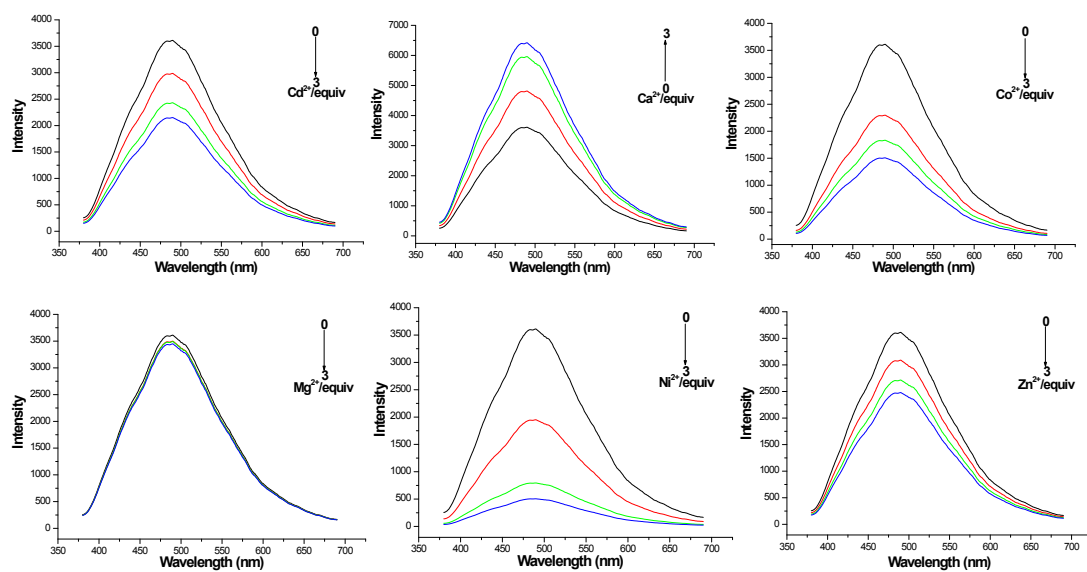


Fig. S14 Emission spectra of complex **1** in DMSO (5×10^{-4} M) at room temperature (excited at 400 nm) in the presence of 0-3 equiv of Cd²⁺ (top left), Ca²⁺ (top middle), Co²⁺ (top right), Mg²⁺ (bottom left), Ni²⁺ (bottom middle), Zn²⁺ (bottom right). Black, no addition; red, 1 equiv; green, 2 equiv; blue, 3 equiv.

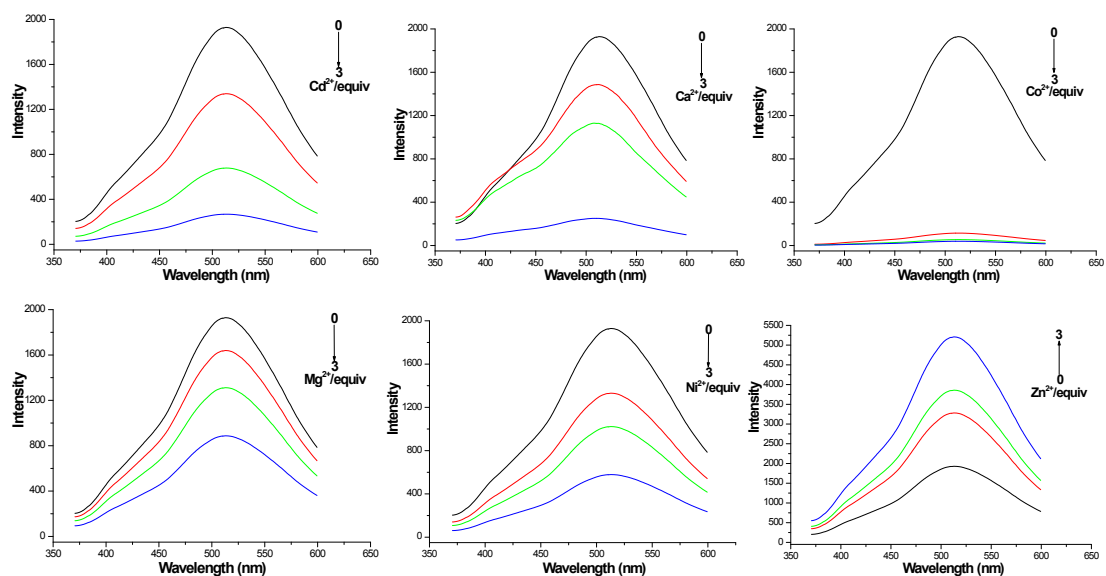
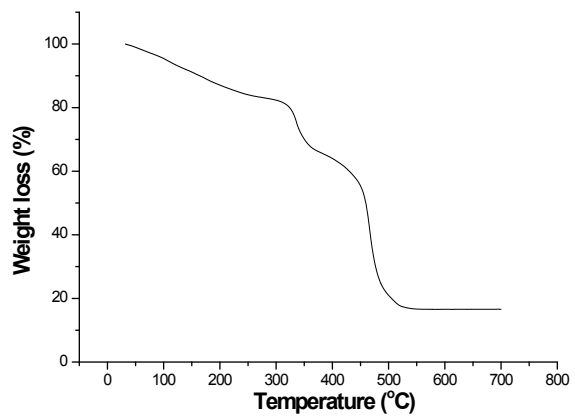
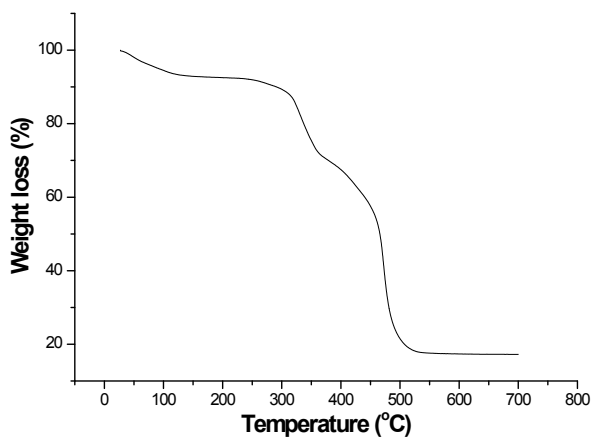


Fig. S15 Emission spectra of complex **1a** in DMSO (5×10^{-4} M) at room temperature (excited at 400 nm) in the presence of 0-3 equiv of Cd²⁺ (top left), Ca²⁺ (top middle), Co²⁺ (top right), Mg²⁺ (bottom left), Ni²⁺ (bottom middle), Zn²⁺ (bottom right). Black, no addition; red, 1 equiv; green, 2 equiv; blue, 3 equiv.



a)



b)

Fig. S16 TGA trace of **1** for a) and **1a** for b).

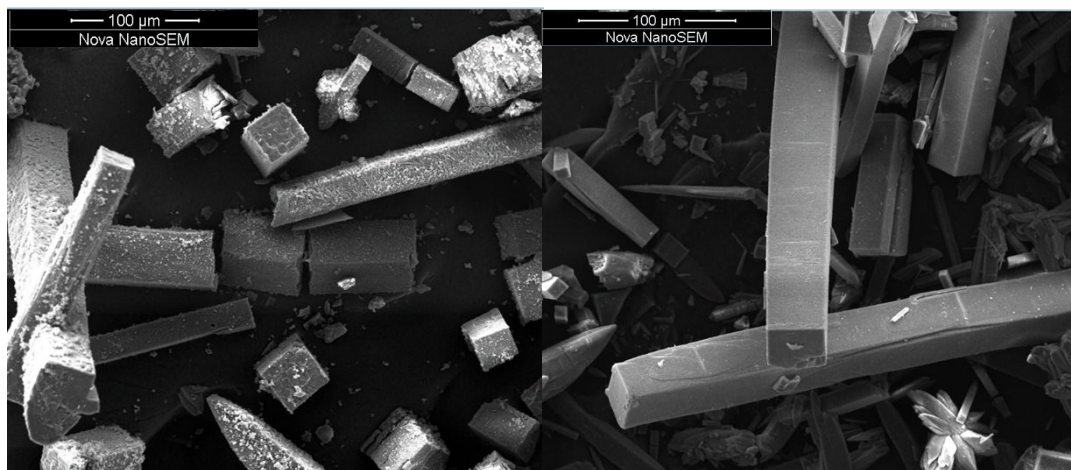


Fig. S17 SEM images of complex 1.

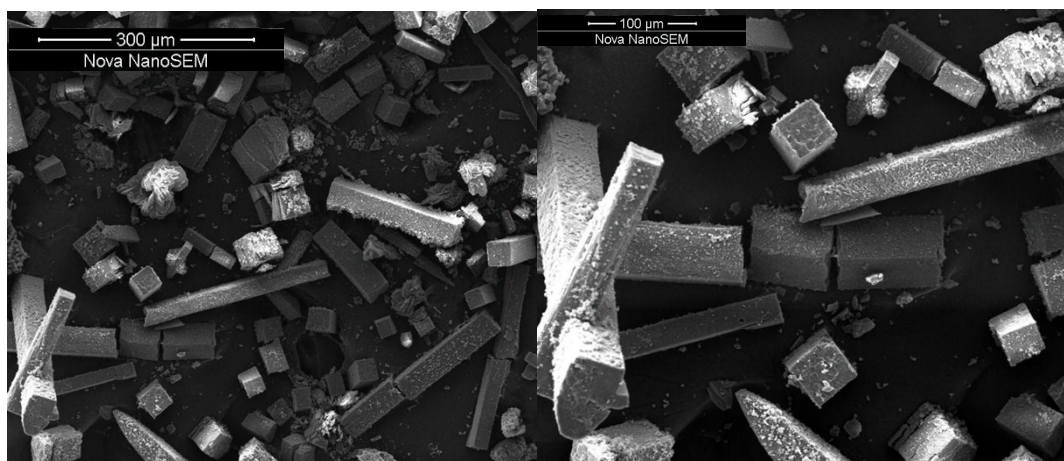


Fig. S18 SEM images of complex **1a**.

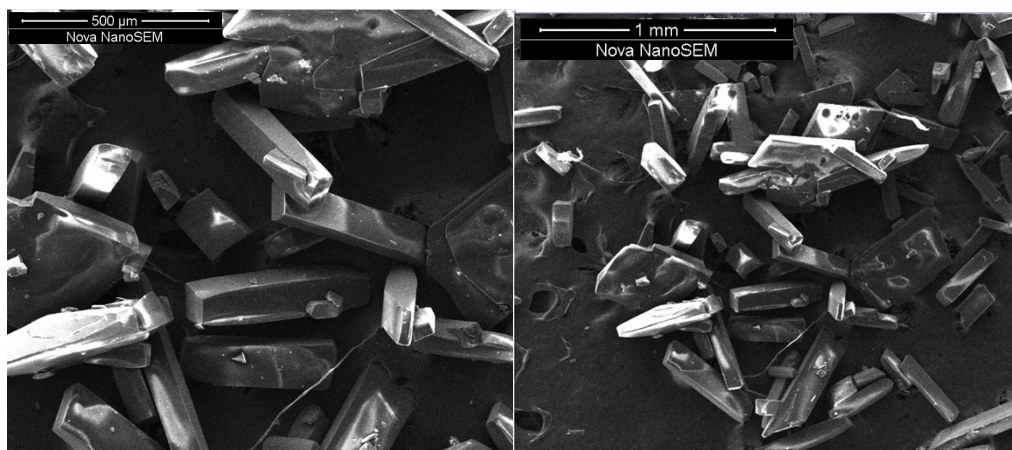


Fig. S19 SEM images of complex **1b**.